IJRCS

International Journal of Robotics and Control Systems
Vol. 5, No. 5, 2025, pp. 2379-2398
ISSN 2775-2658
http://pubs2.ascee.org/index.php/ijrcs

ASCEE

Design and Fabrication of a 6-DOF Articulated Robotic Arm for Research and Educational Applications

Van Tho Nguyen [a,1,*], Thanh Quyen Ngo [a,2], Mien Ka Duong [a,3]

[a] Faculty of Electrical Engineering Technology, Industrial University of Ho Chi Minh City, No. 12 Nguyen Van Bao, Hanh Thong Ward, Ho Chi Minh City, Vietnam
[1] nguyenvantho@iuh.edu.vn; [2] ngothanhquyen@iuh.edu.vn; [3] duongmienka@iuh.edu.vn
* Corresponding Author

ARTICLE INFO

Article history
Received July 06, 2025
Revised September 15, 2025
Accepted November 14, 2025

Keywords
6-DOF Robotic Arm;
Design and Fabrication;
Forward Kinematics;
Structural Analysis;
SolidWorks Design;
Inverse Kinematics

ABSTRACT

Robotics has become increasingly integral to modern life and industrial production, making hands-on experience with physical models essential for students of automation. This paper details the mechanical design and fabrication of a low-cost 6-DOF articulated robotic arm, specifically developed for university-level educational and research applications. The mechanical structure was developed using SolidWorks software and verified through Finite Element Analysis (FEA) to ensure structural rigidity. FEA simulations showed a maximum stress of 0.3095 MPa at the connection between Link 3 and Link 4, confirming the structural integrity of the design under applied loads without failure. The robotic arm offers a maximum reach of 1.045 m, and a horizontal stroke of 0.775 m. Kinematic parameters were directly derived from the mechanical design drawings, supporting both forward and inverse kinematic analyses. A prototype was fabricated using CNC machining to validate the feasibility of the mechanical design. Experimental evaluation for pick-and-place tasks demonstrated acceptable accuracy and repeatability at low and medium speeds, with an average deviation of approximately ±0.5 mm. When operating with a 1 kg load, Joint 5 exhibited a significant increase in tracking error to 10.455×10^{-3} rad, compared to 5.027×10^{-3} rad without a load. Despite good stability, current limitations include low operating speed and restricted payload capacity, with noticeable vibration under heavier loads, suggesting areas for future enhancement.

1. Introduction

Automation revolution is driving a sharp increase in the need for robotic manipulators. The integration of AI, machine learning and advanced sensors is broadening the application of robotic manipulators across industries, from manufacturing and healthcare to research and entertainment [1]. Their inherent advantages—stability, accuracy, speed, and high reliability—position them as indispensable components in modern industrial automation [2]. Furthermore, the capacity to reduce labor costs, perform tasks in hazardous environments, and operate continuously renders robotic manipulators a compelling solution for numerous enterprises [3]-[5]. More than just saving time and resources, robotic manipulators play an important role in promoting innovation and competitive advantage in an increasingly automated market.

Robotic manipulators are electromechanical devices that replicate human arm movements [6]. They can operate independently to perform specific tasks or as part of a larger robotic system [7]-[9] Typically, they consist of 3 segments: from the shoulders to the elbows, from the elbows to the wrists and finally a hand-like part called the end-effector mechanism [10]. Industrial manipulators can perform tasks such as material loading and unloading, component assembly, automatic welding, and coating with much higher accuracy and speed than human capabilities [11]. A key specification of a robotic arm is its degrees of freedom (DOFs), which is the number of ways it can move freely. Basic designs utilize 3 to 4 DOFs [12]-[16], which are well-suited for repetitive tasks that require limited flexibility, such as basic pick-and-place operations. More common in industry are robot arms with 5 or 6 DOFs [17]-[21], which allow the robot arm to move in three directions and rotate around three axes to perform complex tasks like welding, painting, or assembly. For applications requiring extreme precision and adaptability, complex robot designs can even exceed 15 DOFs or more [22]-[24]. In [25], it presented two new designs of manipulator robots for construction purposes; one is for transporting construction materials, and the other is for supporting printing with concrete mixtures. The two robot manipulator models are designed to address the current problem of expanding the application of 3D printing in construction engineering. Previous research on robotic manipulators has explored various configurations and manufacturing methods. Some studies, for instance, focused on manipulators with fewer DOFs, such as 2-DOF articulated designs for assembly tasks by Khalid et al. [26] or 3-DOF manipulators for lifting by Shutnan et al. [12], which primarily remained in simulation environments without fabrication. This lack of physical implementation limits practical validation and understanding of operational performance. Among those that did proceed to manufacturing, such as a 4-DOF articulated manipulator by Vaheed et al. [27] or a 3-DOF pick-and-place robot designed and manufactured by Kariuki et al. [28], errors in object detection, accuracy, and repeatability were reported, highlighting challenges in achieving consistent performance.

Furthermore, the choice of actuators and controllers often introduced complexity. A controller acts as the central processor, serving as the brain of a robotic arm. It executes all operations, from simple movements to complex tasks, from manual joggings to fully programmed automatic tasks. Therefore, the controller is a critical component to consider during the design of a robotic arm. While some designs, such as a 4-DOF manipulator developed by Mustaffa et al. [29] and a 5-DOF feeding manipulator designed by Kruthika et al. [30], utilized DC motors, these typically necessitated additional interfacing circuits like H-bridges to connect with microcontrollers. Similarly, Ahmed et al. employed stepper motors which required specific motor drives and presented difficulties in modifying their speed. In contrast, the study by Sharkawy and Nazzal, which developed a 5-DOF manipulator for industrial tasks, emphasized the use of servo motors for their ease of programming and direct connection to control units like the Arduino Uno, thereby avoiding the need for complex interfacing [31]. Their work also notably leveraged 3D printing technology with plastic materials to produce accurate, lightweight, and cost-effective parts. This approach allowed for a highly repeatable pick-and-place task for known environments without external sensors. However, this design was limited by its fewer DOFs, which made it unsuitable for complex tasks. The use of plastic materials also introduced issues with friction during movement, as well as changes related to temperature effects on part dimensions and end-effector durability. In [32], a microcontroller based system was utilized to control a light-weight 6-DOF robotic arm equipped with a mobile robot. In addition to microcontrollers, PLCs are also one of the most used controllers to control robotic manipulators [33]-[36]. However, the processing and memory capabilities of the Arduino Uno are still limited, while PLCs are expensive. Conversely, PC-based controllers offer a versatile alternative for simultaneously controlling multi-DOF robotic arms [37]-[43]. These controllers, with their self-developed interfaces and high customization capabilities, easily integrate complicated control methods and allow for expansion of control axes. Users can readily program and adjust control commands, which significantly improves flexibility and meets diverse operational requirements.

In addition, the ability to grasp and manipulate objects, determined by the end-effector, is also crucial to the design of a robotic arm [44]-[48]. The end-effector, a custom-designed part attached to the manipulator arm, typically functions as a gripper, a tool, or sometimes even a complex hand-like

mechanism. End-effectors are classified depending on design, power source, and application. While industrial grippers often use hydraulic, pneumatic, or electric power, electromagnetic grippers are increasingly favored in manufacturing for their precise handling of irregularly shaped objects [44], [49], [50]. These electromagnetic grippers offer advantages over pneumatic and electric alternatives; electric grippers tend to be heavier, impacting speed and flexibility, whereas pneumatic grippers require large cylinders that impact space and aesthetics.

The primary contribution of this study is the comprehensive design and fabrication of a low-cost 6-DOF articulated manipulator, intended for research and educational applications at the university level. Unlike previous studies that focused on lower DOF configurations with limited workspace flexibility, this research achieves enhanced operational efficiency through a 6-DOF configuration with 1045 mm maximum reach and 775 mm horizontal stroke, significantly expanding the working envelope compared to lower DOF designs discussed in literature. The mechanical structure of the manipulator was rigorously designed using SolidWorks and fabricated with CNC machining from Aluminum Alloy 6061. This material selection and manufacturing process ensures superior structural rigidity, enhanced durability against operational stresses, and reliable load handling, as validated by comprehensive Finite Element Analysis (FEA) simulations. In addition, our study goes beyond demonstrating basic operational effectiveness by conducting extensive experimental validation to precisely evaluate the operating range, accuracy, repeatability, speed and load capacity. This platform facilitates the application of theoretical concepts to practical problem-solving in teaching. The remainder of the paper is organized as follows: Section 2 details the mechanical design of the 6-DOF robotic arm; Section 3 describes its kinematics; Section 4 presents the control methodology; Section 4.2 details model testing and evaluation; and Section 5 concludes with future development direction.

2. Mechanical Design

2.1. Design Objective

Designing a robotic arm with human-like functionality is a complex mechanical engineering challenge, requiring careful consideration of structural integrity, material selection, and flexibility [51]-[54]. This study focuses on developing a 6-DOF articulated robotic arm with a 1045 mm reach and 775 mm horizontal stroke. The kinematic parameters of the robotic arm are d_1 = 315 mm, a_2 = 318 mm, d_3 = 80 mm, d_4 = 312 mm, and d_5 = 170 mm. The detailed designs of the robotic arm were generated using SolidWorks software with technical specifications summarized in Table 1.

Table 1. The technical specifications of the 6-DOF robotic arm

Items			
Axes	6		
Weight	26.2 kg		
Payload	1.0 kg		
Maximum reach	1.045 m		
Horizontal stroke	0.775 m		
Drive method	AC servo motors (Delta series)	J1	400W
		J2	400W
		J3	200W
		J4	100W
		J5	100W
		J6	100W
Sensors	Absolute serial encoders		
Brakes	Electric brakes		
Motion controller	Mach3 CNC Controller		
Power	220V AC, 50/60Hz		

2.2. CAD Designing

Joint 1, illustrated in Fig. 1, is a crucial component for the robotic arm, providing both stability and rotational mobility. Stability is achieved through a wide, flat surface (Fig. 1 a) that ensures the

arm remains balanced. Furthermore, Joint 1 integrates a power transmission system consisting of a timing belt and rolling element bearing (Fig. 1 b), which increases torque and ensures smooth, stable operation. The manufactured and assembled base, after CNC machining, is shown in Fig. 1 c, demonstrating the realization of the design.

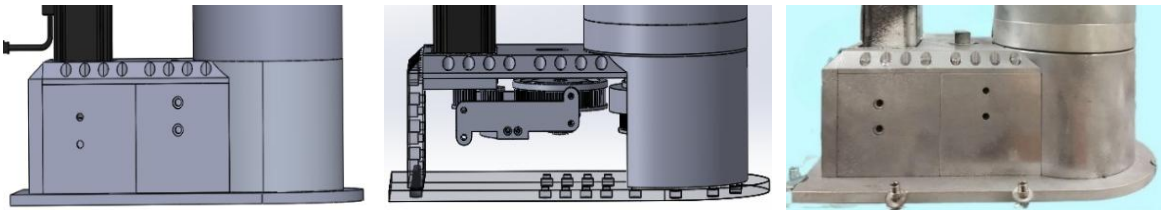

(a) (b) (c)

Fig. 1. Mechanical design of Joint 1, (a) CAD design of the base, (b) transmission system, and (c) the prototype of the base

As shown in Fig. 2, Joint 2 employs a rotating mechanism, rigidly affixed to the base via bolts, to achieve rotational motion around the Z-axis. To ensure adequate torque for accurate positioning, a planetary gearbox is integrated between the joint and its servo motor.

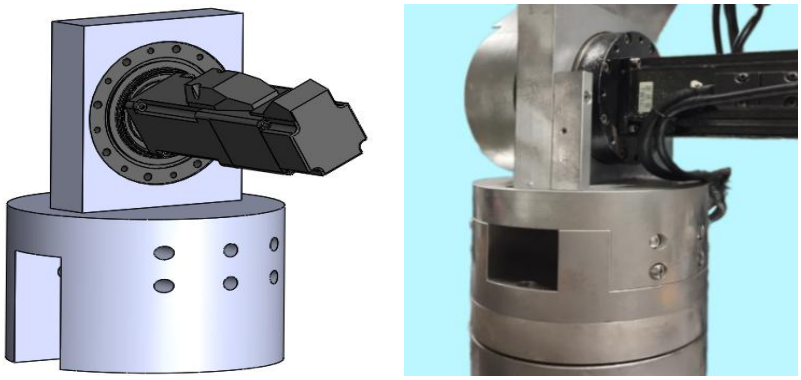

(a) (b)

Fig. 2. Mechanical design of Joint 2, (a) CAD design of Joint 2, and (b) The prototype of Joint 2

Link 2, illustrated in Fig. 3, serves as a rigid structural connection between Joints 2 and 3, facilitating vertical (up/down) and horizontal (forward/backward) displacement of the manipulator. These movements define the working range and enhance accessibility. Aluminum was chosen as the link material, consistent with other links, due to its favorable combination of strength and low density, which supports operational forces while minimizing inertia.

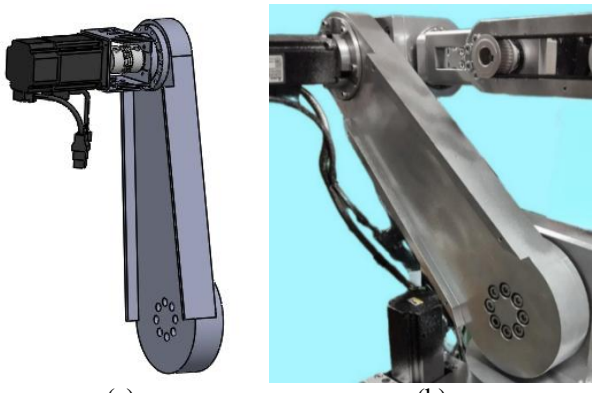

(a) (b)

Fig. 3. Mechanical design of Link 2 and Joint 3, (a) CAD design, and (b) The prototype

As shown in Fig. 4 and Fig. 5, Joints 4 and 5 are interconnected through a link offset, providing the robotic arm with the degrees of freedom necessary for complex and precise manipulation.

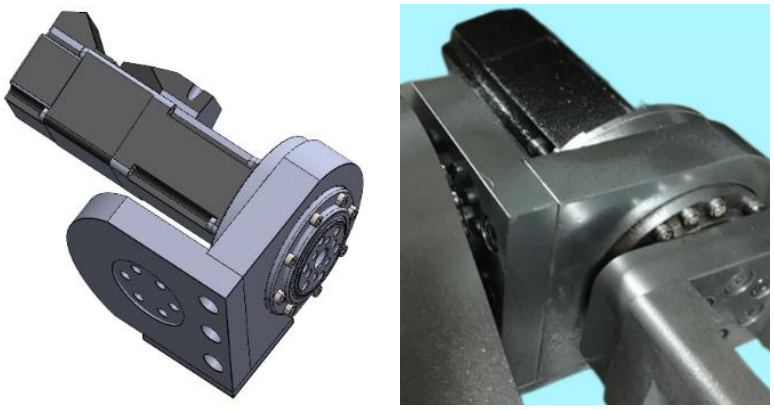

(a) (b)

Fig. 4. Mechanical design of Joint 4, (a) CAD design, and (b) The prototype

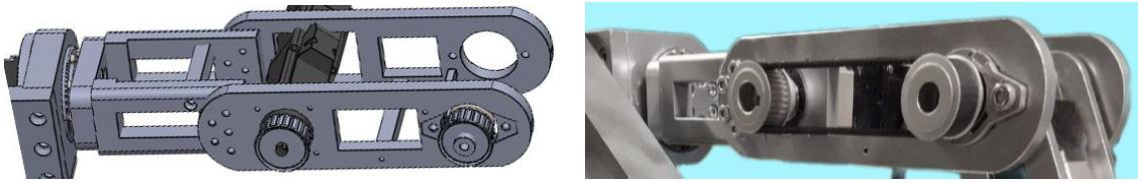

(a) CAD model of Joint 5 (b) The prototype of Joint 5

Fig. 5. Mechanical design of Joint 5

The robot end-effector is augmented with an electromagnetic gripper, attached at Joint 6 (Fig. 6) to facilitate metallic object interaction. Upon activation, the electromagnet generates a sufficient holding force for object manipulation during movement and task execution. The design allows for scaling the number of magnets to accommodate varying load demands, determined through pre-calculations.

Fig. 7 presents the complete design of the 6-DOF robotic arm, including joints and links that enable flexible movement within the workspace. Accompanying the arm is an end-effector mechanism, specifically designed for metal-based pick-and-place applications, which significantly enhances the versatility of the system. Fig. 8 provides further detail on the motion by outlining each rotational joint of the manipulator and clearly indicating the rotation direction of each joint. This clarity is crucial for kinematic analysis, trajectory planning, and jogging control, making it easier for students to visualize the complex motion mechanisms of a multi-degree-of-freedom manipulator can perform.

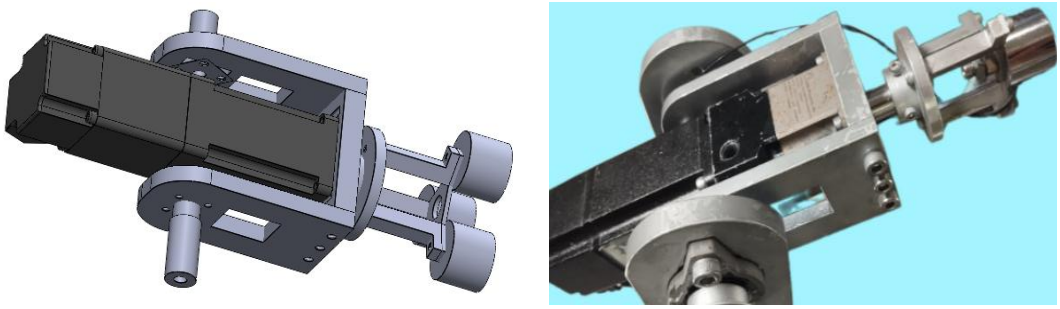

(a) CAD model of Joint 6 and end-effector (b) The prototype after CNC machining

Fig. 6. Mechanical design of Joint 6, (a) CAD design of Joint 6 and end-effector, and (b) The prototype after CNC machining

2.3. Material Selection

The material selection for a 6-DOF robotic manipulator is governed by critical design factors, including durability against repeated operational and environmental stresses, strength for reliable load

handling without deformation, minimal weight for high dynamic performance and energy efficiency, and reasonable cost. Aluminum alloy 6061 satisfies these demands with its excellent strength-to-weight ratio, resistance to wear, and ease of CNC machining, while maintaining structural stiffness. This selection ensures the manipulator can handle its maximum payload without failure, resist wear, and allow for the efficient fabrication of complex parts. The detailed material properties of Aluminum Alloy 6061 are presented in Table 2.

Table 2. Aluminum 6061 properties

Items	Metric
Tensile Yield Strength	290 MPa
Elongation at Break	12-17%
Hardness, Brinell	95
Modulus of Elasticity	68.9 GPa
Density	2.7 g/cc

3. Kinematic Modelling of the Robotic Arm

The kinematics model of the designed 6-DOF robotic manipulator involves a comprehensive understanding of the intricate relationship between the joint parameters and the pose of the robot end-effector. This model is crucial for accurately controlling the movements of the end-effector and ensuring precise task execution. The geometry configuration of the robotic arm, which includes the arrangement and interaction of its joints and links, is depicted in Fig. 9. This figure provides a clear visual representation of the mechanical structure of the arm, which is fundamental to the kinematic analysis and control design.

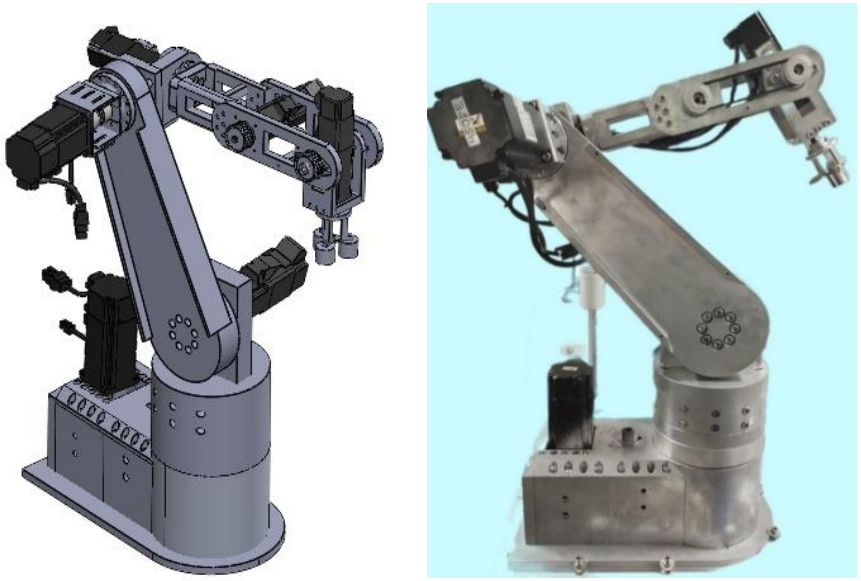

(a) (b)

Fig. 7. The complete design of 6-DOF robotic arm, (a) CAD design and (b) The prototype of the 6-DOF robotic arm

3.1. Forward Kinematics

Forward kinematics aims to determine the position and orientation of the end-effector with respect to a reference frame based on the given joint parameters. In this study, the forward kinematics of the proposed 6-DOF robotic arm is analyzed using the Denavit-Hartenberg (D-H) convention [55]. This convention establishes coordinate frames attached to each joint, utilizing four parameters: link length (a_i), twist angle (α_i), link offset (d_i), and joint angle (θ_i). The assigned coordinate frames for each robot joint are illustrated in Fig. 9, and the corresponding D-H kinematic parameters are listed in Table 3.

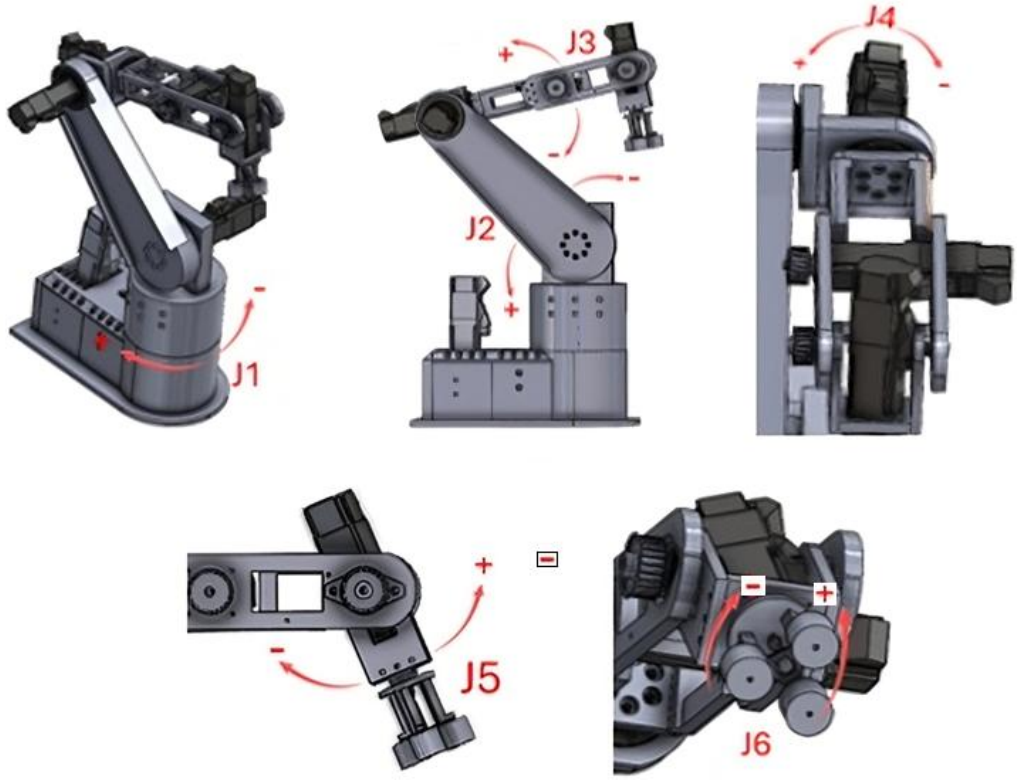

Fig. 8. The rotary joints of the 6-DOF robotic arm

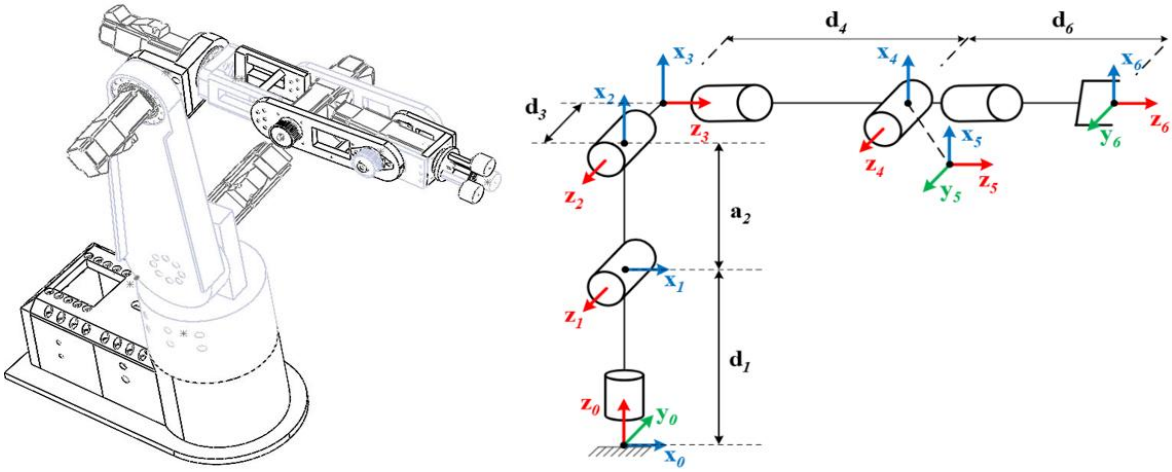

Fig. 9. Rigid body and coordinate frame assignment for the 6-DOF robotic arm

Table 3. The D-H kinematic parameters

Axis	a_i	α_i	d_i	θ_i
1	0	$\pi/2$	d_1	θ_1
2	a_2	0	0	θ_2
3	0	$\pi/2$	d_3	θ_3
4	0	$-\pi/2$	d_4	θ_4
5	0	$\pi/2$	0	θ_5
6	0	0	d_6	θ_6

To compute the position and orientation of the end-effector, the D-H convention utilizes a series of coordinate transformations, which are represented by homogeneous matrices [55]. Then, the overall homogeneous transformation matrix can be easily derived as.

$$T_6^0 = A_1^0 A_2^1 A_3^2 A_4^3 A_5^4 A_6^5 = \begin{bmatrix} r_{11} & r_{12} & r_{13} & p_x \\ r_{21} & r_{22} & r_{23} & p_y \\ r_{31} & r_{32} & r_{33} & p_z \\ 0 & 0 & 0 & 1 \end{bmatrix} \quad (1)$$

where A_1^0, A_2^1, A_3^2, A_4^3, A_5^4, A_6^5 are the transformation matrices between the coordinate frames. The components $r_{ij(i,j=1,2,3)}$ in (1) represent the components of the rotation matrix of Frame *6* with respect to Frame *0*. The position components are determined as.

$$p_x = a_2c_1c_2 + d_3s_1 + d_4c_1s_{23} + d_6[s_5(c_1c_{23}c_4 + s_1s_4) + c_1s_{23}c_5] \quad (2)$$

$$p_y = a_2s_1c_2 - d_3c_1 + d_4s_1s_{23} + d_6[s_5(s_1c_{23}c_4 - c_1s_4) + s_1s_{23}c_5] \quad (3)$$

$$p_z = d_1 + a_2s_2 - d_4c_{23} + d_6(s_{23}c_4s_5 - c_{23}c_5) \quad (4)$$

where $s_{23} \triangleq \sin(\theta_2 + \theta_3)$; $c_{23} \triangleq \cos(\theta_2 + \theta_3)$; $s_{45} \triangleq \sin(\theta_4 + \theta_5)$

3.2. Inverse Kinematics

In contrast to forward kinematics, which involves determining the position and orientation of the end-effector based on known joint parameters, the inverse kinematics problem requires computing the joint parameters given the desired position and orientation of the end-effector. This problem is crucial in robotics because manipulation tasks are typically specified in terms of the end-effector pose. However, this problem is inherently more challenging than forward kinematics due to the non-linear nature of the equations involved and the potential for multiple solutions or no solution at all. Various methods have been developed to address the inverse kinematics problem, including algebraic methods, which involve solving polynomial equations; geometrical methods, which use the spatial relationships between the joints; and iterative methods, which employ numerical techniques to converge on a solution [56]-[63]. Each method has its advantages and limitations, and the choice of method can depend on the specific application and constraints of the robotic system. For the 6-DOF articulated manipulator designed for university-level research and educational applications, the algebraic method is chosen to solve the inverse kinematics problem since it typically allows for a direct, closed-form solution, which offers computational efficiency and deterministic nature, crucial for real-time control implementations. Furthermore, a derivable algebraic solution provides a clearer and more fundamental mathematical understanding of robot kinematics, making it highly suitable for the intended educational purpose of this robotic arm. The calculation of the joint angles ($\theta_1 - \theta_6$) is summarized in the flowchart in Fig. 10.

4. Results and Discussion

4.1. Structural Simulation Analysis of the Designed Manipulator

To assess the robotic long-term durability, SolidWorks Simulation was used to analyze its mechanical structure under defined loads and environmental conditions. Stress simulation is employed to pinpoint areas of concentrated stress or potential failure points, enabling design optimization. The simulation results, illustrated in Fig. 11 b, reveal a maximum stress of 0.3095 MPa at the connection between Link 3 and Link 4. This indicates that the model is capable of withstanding the applied load without failure.

Both displacement and deformation simulations were conducted to evaluate the structural integrity and performance of the design under operational conditions. These simulations aim to ensure that model displacement and deformation remain within acceptable limits. Results, shown in Fig. 11 c (displacement) and Fig. 11 d (deformation), indicate minimal displacement and deformation, respectively. In both cases, the maximum displacement/deformation occurs between Link 5 and Link 6. The simulation analyses confirm that the stress, displacement, and deformation parameters remain

within the allowable limits of the design, thus validating the structural safety and operational viability as an industrial robotic arm.

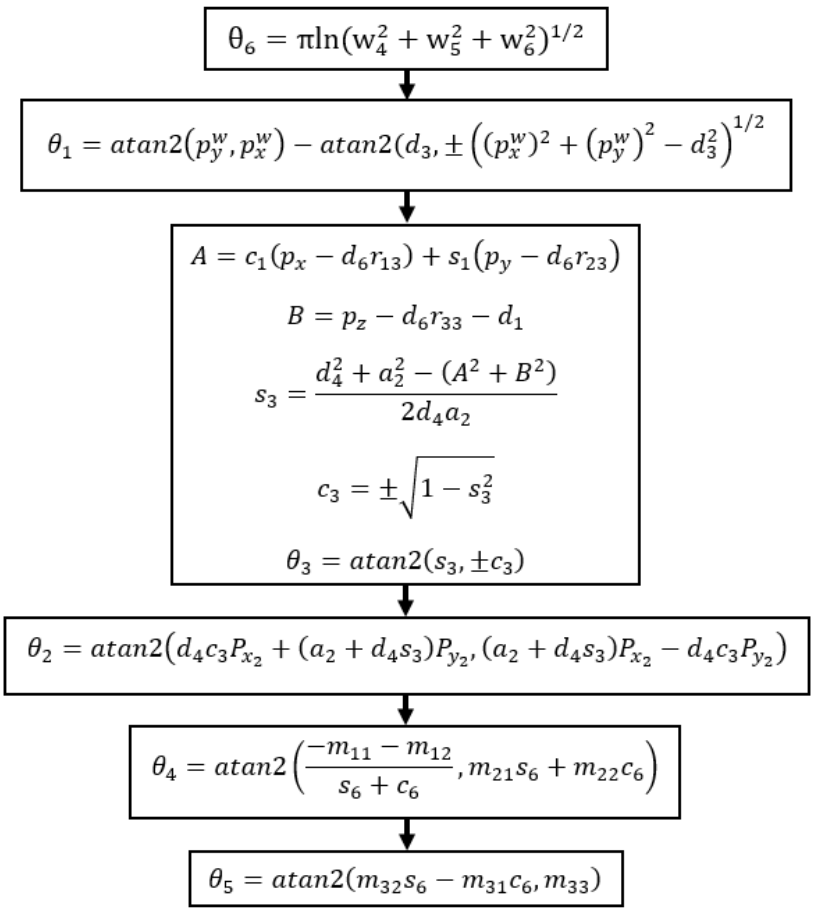

Fig. 10. Algorithm for solving inverse kinematics problem of the 6-DOF robotic arm

4.2. Experimental Results

Experiments were performed in this section to analyze and evaluate the design of the 6-DOF robotic arm based on criteria such as operating range, accuracy, repeatability, speed, and load capacity. Fig. 12, the device connection diagram, illustrates the intricate system architecture that enables precise and synchronized manipulation. At the core of the control strategy is the Mach3 Fly Motion CNC controller, a PC-based system explicitly chosen for its versatility and advanced capabilities in managing multi-degree-of-freedom robotic arms. This type of controller facilitates self-developed interfaces and offers high customization, allowing for the integration of complex control methods and the expansion of control axes to meet diverse operational requirements.

The actuator system, critical for dynamic performance, comprises Delta ECMA motors paired with ASDA-A2 drivers. These AC servo motors, specified for each joint with varying power ratings (Joint 1, Joint 2 at 400W; Joint 3 at 200W; Joint 4, Joint 5, Joint 6 at 100W), were selected for their ability to provide rapid response, high precision, and stable operational performance. Position detection is precisely managed by absolute serial encoders, which provide crucial feedback for accurate trajectory tracking. Complementing this hardware is the computer-based control interface, depicted in Fig. 13. This graphical user interface (GUI) is a pivotal component for real-time control and monitoring, providing users with comprehensive insights into individual axis positions, as well as the overall position and orientation of the end-effector. As shown in its distinct automation and manual modes, the interface significantly simplifies the execution of intricate experiments and facilitates user interaction. For programming and control, the utilization of G-code further enhances user accessibility and modification capabilities.

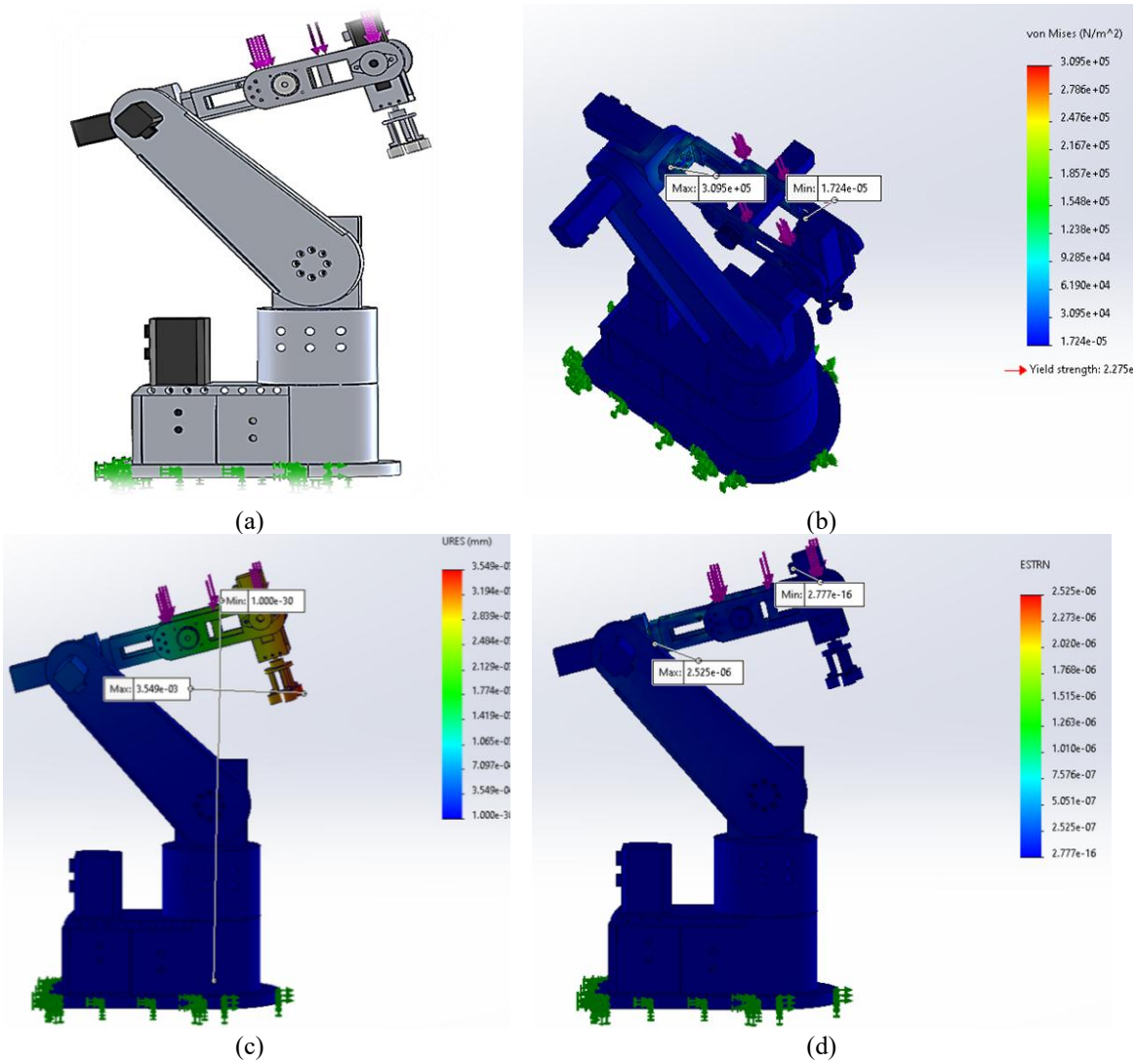

Fig. 11. Structural analysis on design of 6-DOF robotic arm, (a) Setup boundary conditions, (b) Stress simulation result, (c) Displacement simulation result, and (d) Deformation simulation result

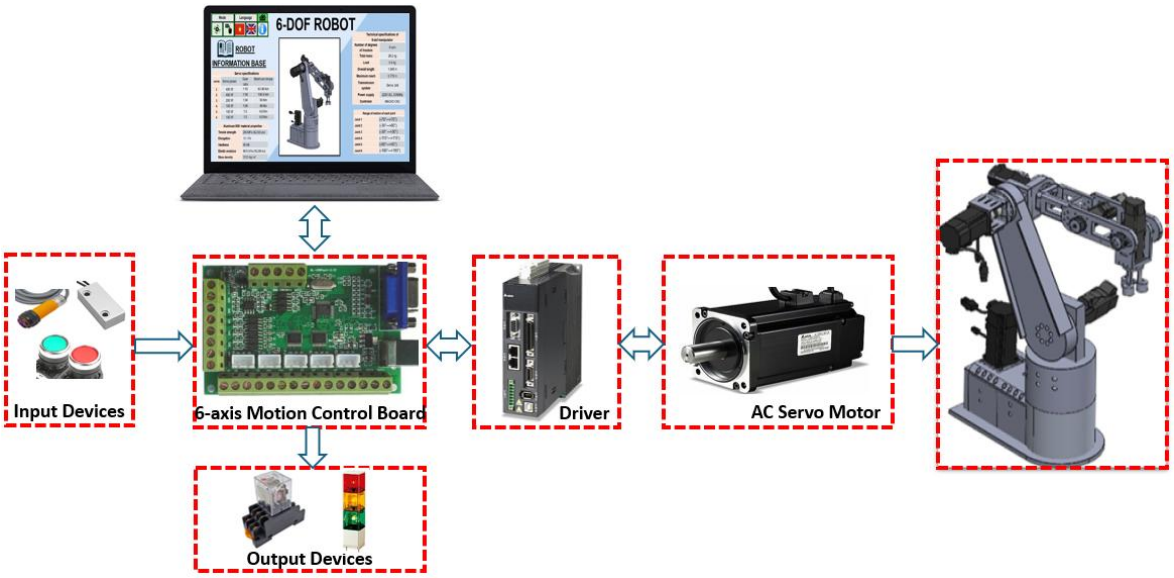

Fig. 12. Device connection diagram

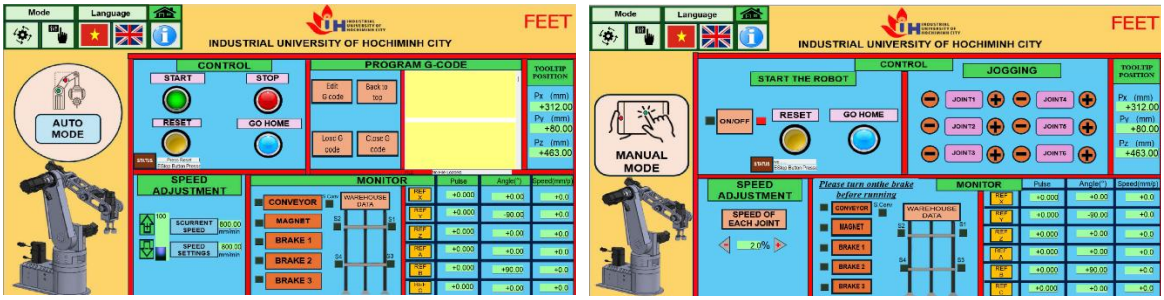

(a) (b)

Fig. 13. Control and monitoring interface, (a) Automation mode, and (b) Manual mode

The workspace of the robotic arm is bounded by its link lengths and individual joint ranges. To determine these boundaries, iterative experiments were performed on each axis with the aid of the control interface, specifically to establish their respective operational limits. Following extensive jogging procedures on individual axes, the operating ranges of the axes, as well as the maximum reach of the robotic arm are summarized in Table 4.

Table 4. The motion range of the manipulator

Items	Metric
Axes	6
Maximum reach	1.045 m
Horizontal stroke	0.775 m
Motion range	Joint 1 -70º/70º
	Joint 2 -30º/60º
	Joint 3 -30º/30º
	Joint 4 -115º/115º
	Joint 5 -60º/40º
	Joint 6 -180º/180º
Drive method	AC servo motors
Position detection	Absolute encoders

To evaluate the performance of the robotic arm for pick-and-place applications, an experiment was carried out. This involved commanding the arm to follow a predefined joint-space trajectory and evaluating the joint tracking error in both no-load and 1 kg load conditions. The trajectory was planned to move from a defined Home position (position A) to a designated object drop-off position in the workspace (position B) over a duration of t_f = 10 seconds. The joint vectors at these two trajectory endpoints were then determined from joint feedback signals, as follows:

$$q_A = [-0.0000, -1.5708, 0.0000, 0.0000, 1.5708, -0.0000]^T \text{ (rad)} \quad (5)$$

$$q_B = [-0.4590, -1.2243, 0.0625, -1.7649, 1.1522, 0.4504]^T \text{ (rad)} \quad (6)$$

For the purpose of achieving smooth motion at the joints, a joint-space polynomial trajectory was planned to control the robotic arm. The equation of motion for each individual joint following a fifth-order polynomial trajectory is determined as follows:

$$\theta_1(t) = -0.0046t^3 + 0.0007t^4 \quad (7)$$

$$\theta_2(t) = -1.5708 + 0.0035t^3 - 0.0005t^4 \quad (8)$$

$$\theta_3(t) = 0.0006t^3 - 0.0001t^4 \quad (9)$$

$$\theta_4(t) = -0.0176t^3 + 0.0026t^4 - 0.0001t^5 \quad (10)$$

$$\theta_5(t) = 1.5708 - 0.0042t^3 + 0.0006t^4 \quad (11)$$

$$\theta_6(t) = 0.0045t^3 - 0.0007t^4 \quad (12)$$

The time-based trajectories of individual joints and the end-effector are presented in Fig. 14 and Fig. 16. Fig. 17 illustrates the no-load joint angle responses, where the solid blue line is the desired trajectory and the red dashed line is the actual trajectory, as measured by encoder feedback. The results indicate good tracking performance for the actual joint trajectories under no-load conditions. Joint 4 shows the minimal error, whereas Joint 5 exhibits the largest error, implying that its belt-driven transmission system contributes to higher inaccuracies compared to other joints.

The responses of individual joint angles when the robotic arm operates with a 1kg load were illustrated in Fig. 18. Under payload, joint errors increase, notably between 3 and 7 seconds. This increased error might be attributed to system lag or poor responsiveness to quick changes in speed. However, the deviation from the designed trajectory remains acceptable, demonstrating the effectiveness of the control system. Tracking error of each individual joint shown in Table 5.

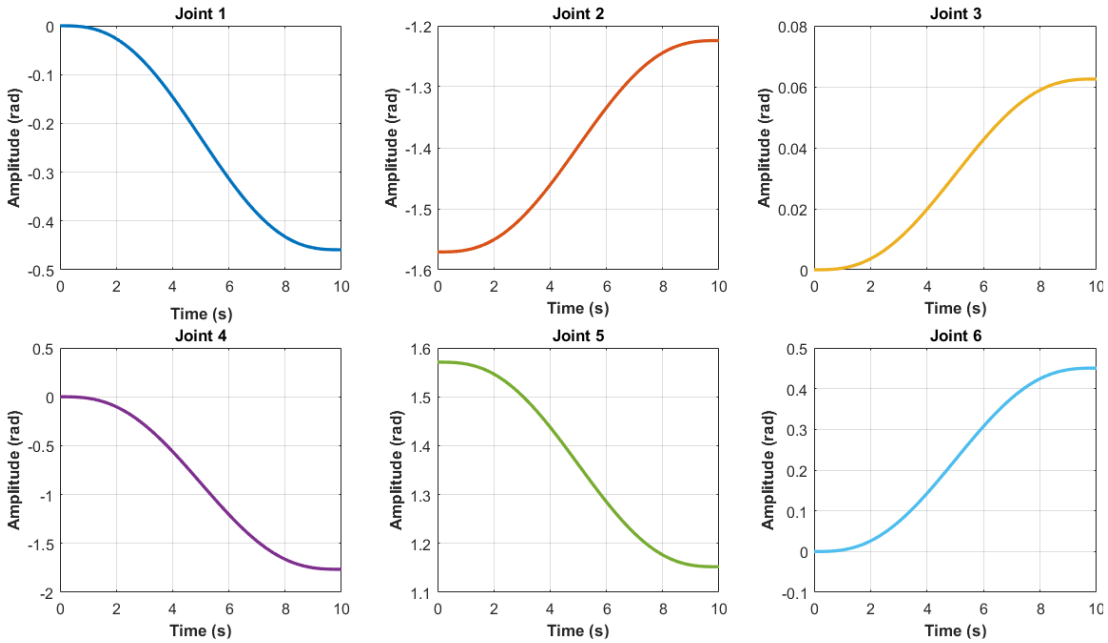

Fig. 14. Desired trajectories of each individual joint

Table 5. Tracking error of each individual joint

Load	RMSE (x10^{-3} rad)					
	Joint 1	**Joint 2**	**Joint 3**	**Joint 4**	**Joint 5**	**Joint 6**
No load	3.142	1.508	1.702	0.503	5.027	4.208
With load	7.854	6.788	3.766	2.263	10.455	7.633

Additionally, repeatability tests were conducted at different speeds. Fig. 19, Fig. 20 show the results for 50 mm/min (low speed), 100 mm/min and 200 mm/min (high speed). The results indicate a relatively small average deviation (within approximately ± 0.5 mm), demonstrating the system maintains stable accuracy. The minimal scatter of data points in Fig. 19 strongly supports the reliable repeatability of the robot arm. However, higher speeds led to increased variance, potentially caused by heightened inertia or mechanical vibrations. This highlights the need for additional calibration or control system optimization to ensure consistent accuracy during high-speed operations.

In summary, the experimental evaluation confirms that the robotic arm exhibits relatively good accuracy and repeatability at low and medium operational speeds. This is underscored by the minimal

deviation between the designed and actual trajectories observed under no-load conditions (Fig. 17), which validates the effective performance of the control system. Specifically, pick-and-place tasks demonstrated acceptable accuracy and repeatability with an average deviation of approximately ±0.5 mm at these speeds, with minimal data scatter at low speeds (Fig. 19). Desired trajectory at the end-effector shown in Fig. 15.

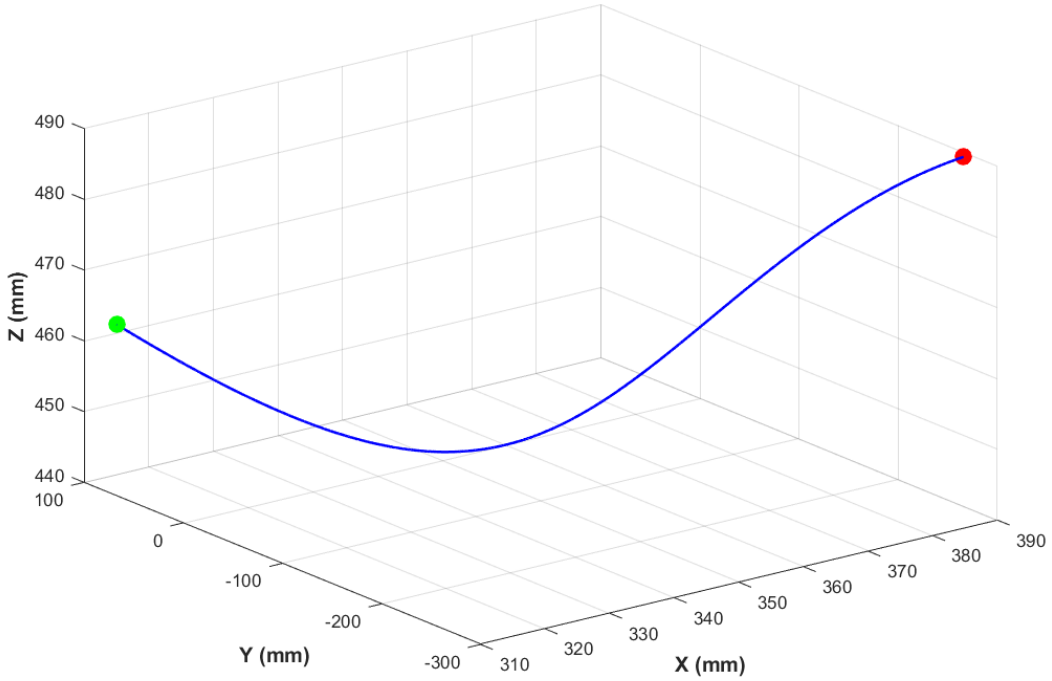

Fig. 15. Desired trajectory at the end-effector

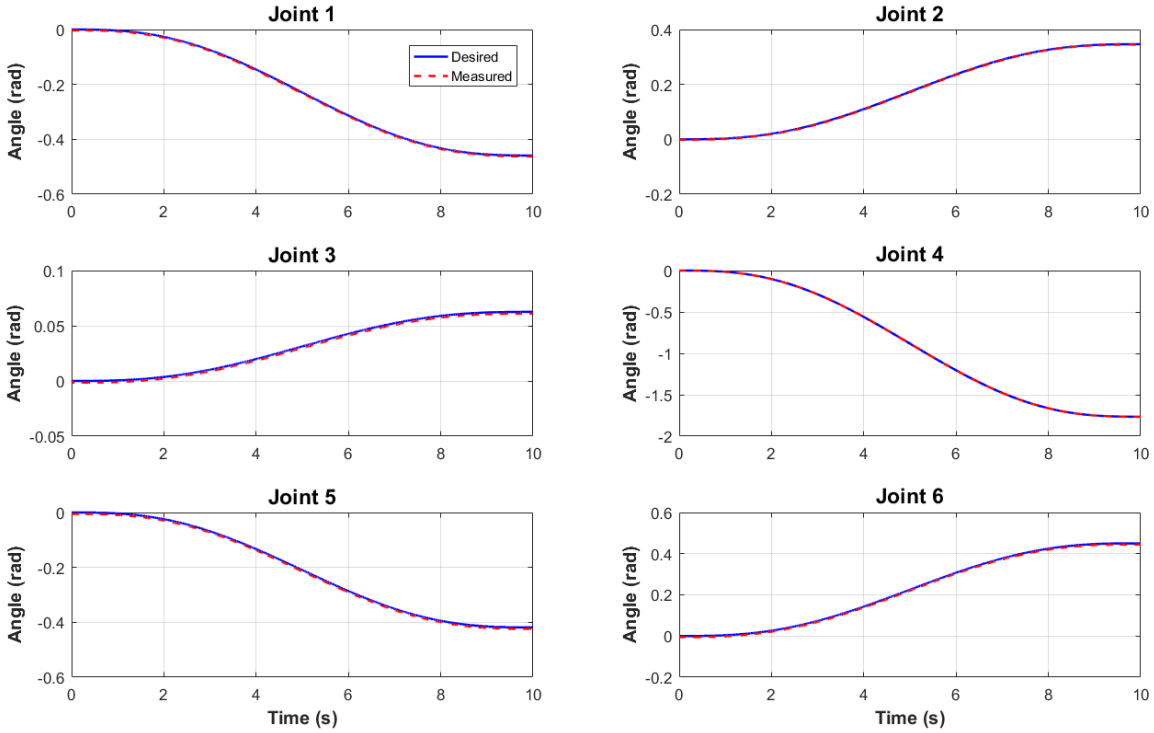

Fig. 16. Trajectory tracking of each joint without load

This provides a crucial experimental foundation, contrasting with the study by He et al. [64], which primarily focuses on the CAD modeling, finite element analysis (FEA), and simulation of

trajectory tracking in MATLAB and Simulink. While He et al. successfully established a mechanical design and simulated performance under loads up to 15N, validating the structural integrity, their work explicitly notes that future endeavors should extend to an experimental platform for an accurate robotic arm and the addition of a trajectory controller. Our study thus fulfills an important gap by providing real-world empirical data on accuracy and repeatability under operational conditions. Despite the demonstrated strengths in accuracy and repeatability at lower speeds, a critical review of our experimental data reveals that the stability and reliability of the system are more nuanced, particularly under dynamic and high-speed conditions. These findings highlight the value of empirical validation and indicate clear areas for future enhancement to ensure consistent accuracy during high-speed and loaded operations.

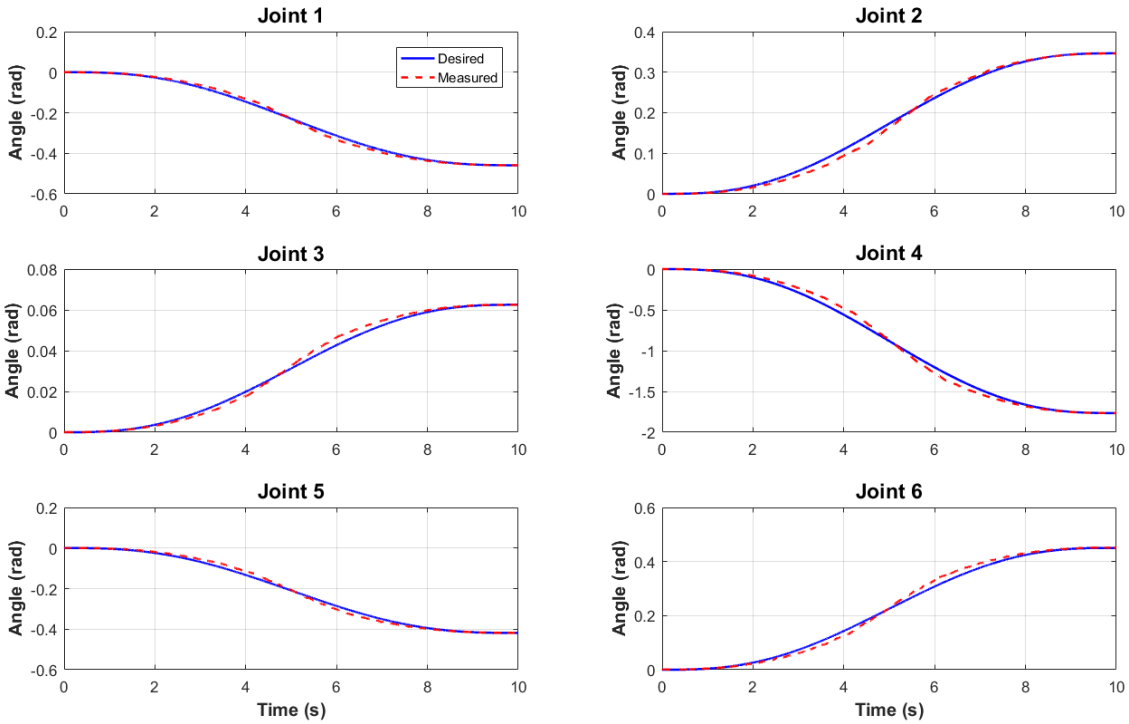

Fig. 17. Trajectory tracking of each joint with load (1 kg)

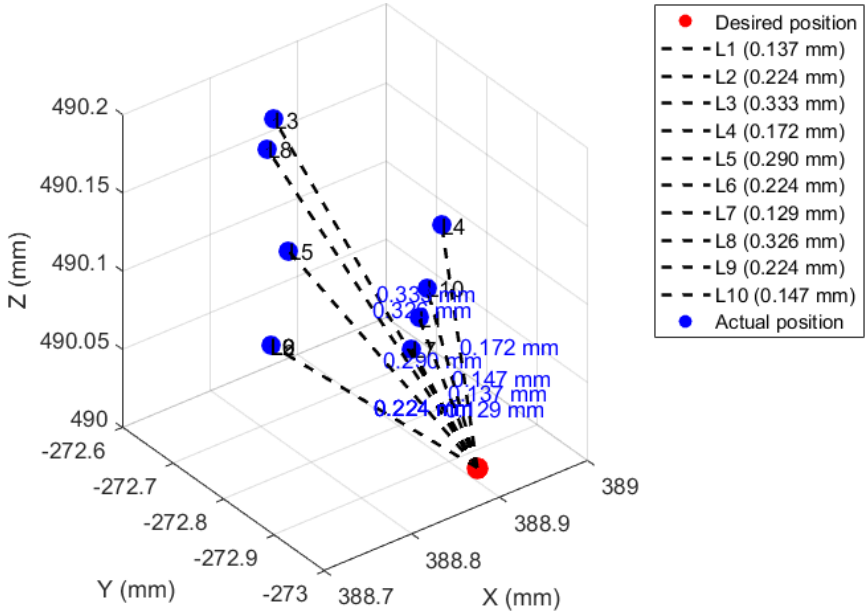

Fig. 18. Repeatability at speed 50 mm/min

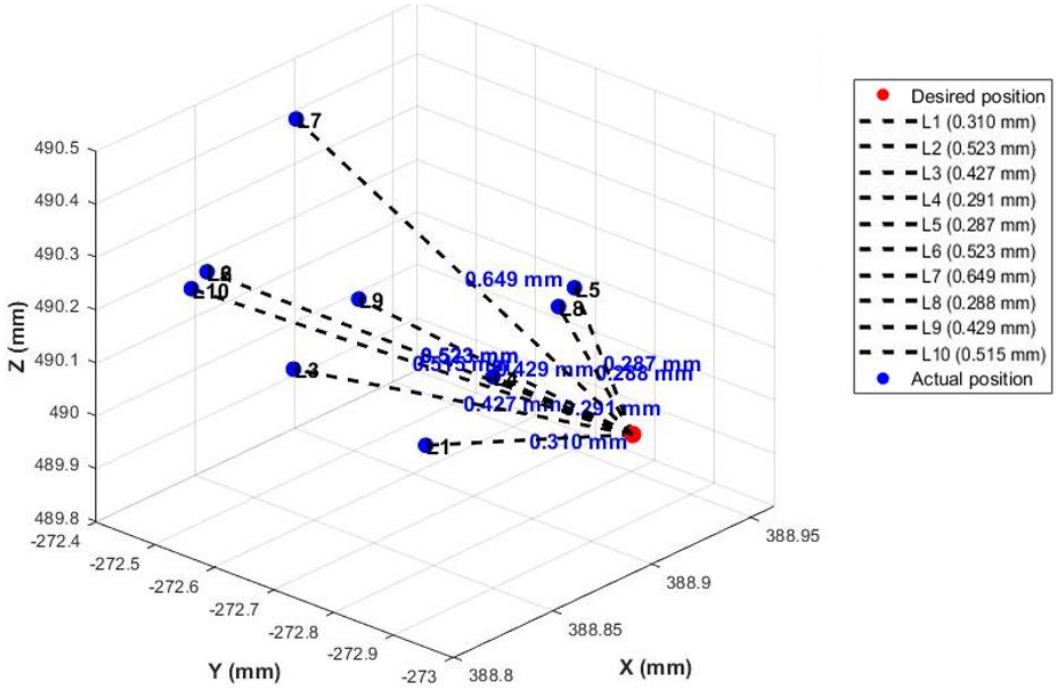

Fig. 19. Repeatability at speed 100 mm/min

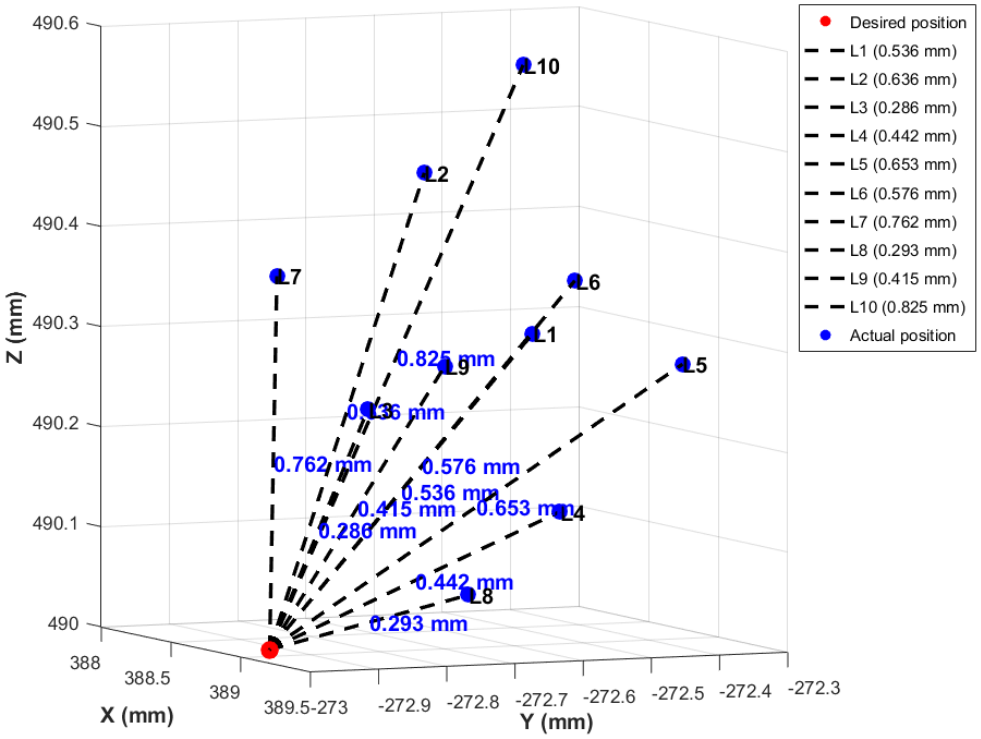

Fig. 20. Repeatability at speed 200 mm/min

5. Conclusions

In conclusion, this research successfully delivered the design and fabrication of a 6- DOF articulated robotic arm, specifically tailored for university-level research and educational applications. The mechanical structure was rigorously developed using SolidWorks and validated through Finite Element Analysis to ensure structural rigidity. The kinematic models of the arm were derived to describe the motion of the end-effector in space. For programming and control, using G-code makes

it easy for users to access and modify. The graphical user interface displays full monitoring and control parameters, facilitating user interaction and robot operation. While initial simulations and no-load experiments showed good tracking performance and acceptable repeatability at low to medium operational speeds, a critical review of the experimental data reveals certain limitations. Contrary to initial assessments of high stability, the system exhibits increased operational errors when subjected to a 1kg load. Specifically, joint tracking errors significantly escalated under load, with RMSE of joint 5 more than doubling from 5.027 to 10.455 $\times 10^{-3}$ rad. This increased variance, particularly at higher speeds, suggests challenges related to heightened inertia and mechanical vibrations. The tendency of the arm to vibrate under heavier loads substantially increases its operational errors, indicating that its stability and reliability are more nuanced than initially stated, especially under dynamic and high-speed conditions. Future work will therefore focus on enhancing the performance of the manipulator under these challenging conditions, this includes

- Optimizing the structural design to increase the payload capacity and reduce vibrations.
- Conducting singularity analysis for safer and more efficient motion planning.
- Implementing advanced calibration techniques to improve overall accuracy and repeatability.
- Developing advanced control algorithms to actively compensate for vibrations and improve tracking accuracy at higher speeds and varying loads.

These advancements will further solidify the role of the robotic arm as a versatile and reliable platform for advanced research and educational applications.

Author Contribution: Van Tho Nguyen was responsible for Conceptualization; Funding acquisition; Formal analysis; Investigation; Methodology; Resources; Simulation; Experiments; Validation; Visualization; Writing – original draft; and Writing – review & editing. **Thanh Quyen Ngo** was responsible for Visualization and Supervision. **Mien Ka Duong** was responsible for Visualization.

Acknowledgment: The authors gratefully acknowledge the financial support funded by the Industrial University of Ho Chi Minh City (IUH), Vietnam through the scientific research program under Contract No. 40/HĐ-ĐHCN, signed on March 03, 2023. We also thank the Faculty of Electrical Engineering Technology (FEET) of IUH for facilitating this research process.

Conflicts of Interest: The authors declare that they have no known competing financial interests or personal relationships that could have appeared to influence the work reported in this paper.

References

[1] R. Shah, A. S. A. Doss, and N. Lakshmaiya, "Advancements in AI-enhanced collaborative robotics: towards safer, smarter, and human-centric industrial automation," *Results in Engineering*, vol. 27, p. 105704, 2025, https://doi.org/10.1016/j.rineng.2025.105704.

[2] W. Wang, Q. Guo, Z. Yang, Y. Jiang, and J. Xu, "A state-of-the-art review on robotic milling of complex parts with high efficiency and precision," *Robotics and Computer-Integrated Manufacturing*, vol. 79, p. 102436, 2023, https://doi.org/10.1016/j.rcim.2022.102436.

[3] B. K. Panda, S. S. Panigrahi, G. Mishra, and V. Kumar, "Chapter Thirteen - Robotics for general material handling machines in food plants," *Transporting Operations of Food Materials Within Food Factories*, pp. 341-372, 2023, https://doi.org/10.1016/B978-0-12-818585-8.00005-2.

[4] T. T. Tung, N. V. Tinh, D. T. P. Thao, and T. V. Minh, "Development of a prototype 6 degree of freedom robot arm," *Results in Engineering*, vol. 18, p. 101049, 2023, https://doi.org/10.1016/j.rineng.2023.101049.

[5] Z. Ali *et al*., "Design and development of a low-cost 5-DOF robotic arm for lightweight material handling and sorting applications: A case study for small manufacturing industries of Pakistan," *Results in Engineering*, vol. 19, p. 101315, 2023, https://doi.org/10.1016/j.rineng.2023.101315.

[6] Y. Lin, H. Zhao, and H. Ding, "Posture optimization methodology of 6R industrial robots for machining using performance evaluation indexes," *Robotics and Computer-Integrated Manufacturing*, vol. 48, pp. 59-72, 2017, https://doi.org/10.1016/j.rcim.2017.02.002.

[7] A. S. Ahmed, H. A. Marzog, and L. A. Abdul-Rahaim, "Design and implement of robotic arm and control of moving via IoT with Arduino ESP32," *International Journal of Electrical and Computer Engineering (IJECE)*, vol. 11, no. 5, pp. 3924-3933, 2021, http://doi.org/10.11591/ijece.v11i5.pp3924-3933.

[8] W. Ji and L. Wang, "Industrial robotic machining: a review," *The International Journal of Advanced Manufacturing Technology*, vol. 103, no. 1, pp. 1239-1255, 2019, https://doi.org/10.1007/s00170-019-03403-z.

[9] N. Robinson, R. Mane, T. Chouhan, and C. Guan, "Emerging trends in BCI-robotics for motor control and rehabilitation," *Current Opinion in Biomedical Engineering*, vol. 20, p. 100354, 2021, https://doi.org/10.1016/j.cobme.2021.100354.

[10] B. Siciliano, L. Sciavicco, V. Luigi, and G. Oriolo, "Robotics: Modelling, planning and control," *Springer*, pp. 1-623, 2009, https://doi.org/10.1007/978-1-84628-642-1.

[11] G. Gulletta, W. Erlhagen, and E. Bicho, "Human-Like Arm Motion Generation: A Review," *Intelligent Robots and Mechatronics*, vol. 9, no. 4, p. 102, 2020, https://doi.org/10.3390/robotics9040102.

[12] W. A. Shutnan *et al*., "Modeling and Control of a 3DOF Robot Manipulator Using Artificial Fuzzy-Immune FOPID Controller," *IEEE Access*, vol. 12, pp. 153074-153088, 2024, https://doi.org/10.1109/ACCESS.2024.3449042.

[13] M. Ayyıldız and K. Çetinkaya, "Comparison of four different heuristic optimization algorithms for the inverse kinematics solution of a real 4-DOF serial robot manipulator," *Neural Computing and Applications*, vol. 27, no. 4, pp. 825-836, 2016, https://doi.org/10.1007/s00521-015-1898-8.

[14] S. Liu, Z.-c. Qiu, and X.-m. Zhang, "Singularity and path-planning with the working mode conversion of a 3-DOF 3-RRR planar parallel manipulator," *Mechanism and Machine Theory*, vol. 107, pp. 166-182, 2017, https://doi.org/10.1016/j.mechmachtheory.2016.09.004.

[15] J. Wu, R.-J. Yan, K.-S. Shin, C.-S. Han, and I. M. Chen, "A 3-DOF quick-action parallel manipulator based on four linkage mechanisms with high-speed cam," *Mechanism and Machine Theory*, vol. 115, pp. 168-196, 2017, https://doi.org/10.1016/j.mechmachtheory.2017.04.012.

[16] L. Zhang, X. Yan, and Q. Zhang, "Design and analysis of 3-DOF cylindrical-coordinate-based manipulator," *Robotics and Computer-Integrated Manufacturing*, vol. 52, pp. 35-45, 2018, https://doi.org/10.1016/j.rcim.2018.02.006.

[17] D. Xu, C. A. Acosta Calderon, J. Q. Gan, H. Hu, and M. Tan, "An analysis of the inverse kinematics for a 5-DOF manipulator," *International Journal of Automation and Computing*, vol. 2, no. 2, pp. 114-124, 2005, https://doi.org/10.1007/s11633-005-0114-1.

[18] V. N. Iliukhin, K. B. Mitkovskii, D. A. Bizyanova, and A. A. Akopyan, "The Modeling of Inverse Kinematics for 5 DOF Manipulator," *Procedia Engineering*, vol. 176, pp. 498-505, 2017, https://doi.org/10.1016/j.proeng.2017.02.349.

[19] X. Wang, D. Zhang, C. Zhao, H. Zhang, and H. Yan, "Singularity analysis and treatment for a 7R 6-DOF painting robot with non-spherical wrist," *Mechanism and Machine Theory*, vol. 126, pp. 92-107, 2018, https://doi.org/10.1016/j.mechmachtheory.2018.03.018.

[20] L. Villaverde, D. Maneetham, "Kinematic and Parametric Modeling of 6DOF(Degree-of-Freedom) Industrial Welding Robot Design and Implementation," *International Journal of Technology*, vol. 15, no. 4, pp. 291-319, 2024, https://doi.org/10.14716/ijtech.v15i4.6559.

[21] R. Zhao, Z. Shi, Y. Guan, Z. Shao, Q. Zhang, and G. Wang, "Inverse kinematic solution of 6R robot manipulators based on screw theory and the Paden–Kahan subproblem," *International Journal of Advanced Robotic Systems*, vol. 15, no. 6, 2018, https://doi.org/10.1177/1729881418818297.

[22] D. Yan *et al*., "CasiaHand: Design and Evaluation of a 15-DoF Tendon-Driven Anthropomorphic Robotic Hand," *IEEE Robotics and Automation Letters*, vol. 10, no. 5, pp. 5026-5033, 2025, https://doi.org/10.1109/LRA.2025.3555161.

[23] A. Bicchi, "Hands for dexterous manipulation and robust grasping: a difficult road toward simplicity," *IEEE Transactions on Robotics and Automation*, vol. 16, no. 6, pp. 652-662, 2000, https://doi.org/10.1109/70.897777.

[24] N. Elangovan, G. Gao, C. -M. Chang and M. Liarokapis, "A Modular, Accessible, Affordable Dexterity Test for Evaluating the Grasping and Manipulation Capabilities of Robotic Grippers and Hands," *2020 IEEE International Symposium on Safety, Security, and Rescue Robotics (SSRR)*, pp. 304-310, 2020, https://doi.org/10.1109/SSRR50563.2020.9292571.

[25] M. H. Ali, Y. Kuralbay, A. Aitmaganbet, and M. A. S. Kamal, "Design of a 6-DOF robot manipulator for 3D printed construction," *Materials Today: Proceedings*, vol. 49, pp. 1462-1468, 2022, https://doi.org/10.1016/j.matpr.2021.07.228.

[26] K. Khalid, A. A. Zaidi and Y. Ayaz, "Optimal Placement and Kinematic Design of 2-DoF Robotic Arm," *2021 International Bhurban Conference on Applied Sciences and Technologies (IBCAST)*, pp. 552-559, 2021, https://doi.org/10.1109/IBCAST51254.2021.9393255.

[27] H. Kareemullah, D. Najumnissa, M. M. Shajahan, M. Abhineshjayram, V. Mohan, and S. A. Sheerin, "Robotic Arm controlled using IoT application," *Computers and Electrical Engineering*, vol. 105, p. 108539, 2023, https://doi.org/10.1016/j.compeleceng.2022.108539.

[28] S. Kariuki, E. Wanjau, I. Muchiri, J. Muguro, W. Njeri, and M. Sasaki, "Pick and Place Control of a 3-DOF Robot Manipulator Based on Image and Pattern Recognition," *Machines*, vol. 12, no. 9, p. 665, 2024, https://doi.org/10.3390/machines12090665.

[29] M. Mustaffa, R. L. Ahmad Shauri, M. Roslan, and M. Idris, "Development of a 4-DOF Robotic Arm: Prototype Design," *International Journal of Engineering & Technology*, vol. 7, pp. 429-432, 2018, https://doi.org/10.14419/ijet.v7i4.18.21983.

[30] K. Kruthika, B. M. Kiran Kumar and S. Lakshminarayanan, "Design and development of a robotic arm," *2016 International Conference on Circuits, Controls, Communications and Computing (I4C)*, pp. 1-4, 2016, https://doi.org/10.1109/CIMCA.2016.8053274.

[31] A.-N. Sharkawy and J. M. Nazzal, "Design and Manufacturing Using 3D Printing Technology of A 5-DOF Manipulator for Industrial Tasks," *International Journal of Robotics and Control Systems*, vol. 4, no. 2, pp. 893-909, 2024, http://dx.doi.org/10.31763/ijrcs.v4i2.1456.

[32] A. Swamardika, I. N. Budiastra, N. Setiawan, N. IndraEr, , "Design of Mobile Robot with Robotic Arm Utilising Microcontroller and Wireless Communication," *International Journal of Engineering and Technology*, vol. 9, no. 2, pp. 838-846, 2017, https://dx.doi.org/10.21817/ijet/2017/v9i2/170902170.

[33] H. Şahin, R. Güntürkün, O. Hız, "Design and Application of Plc Controlled Robotic Arm Choosing Objects According to Their Color," *Electronic Letters on Science and Engineering*, vol. 16, no. 2, pp. 52-62, 2020, https://dergipark.org.tr/en/pub/else/issue/58236/789626#article_cite.

[34] Y. Toporovsky, H. Lawrence, and T. Sobh, "Integration of Vision System, Intelligent ROBO Actuator, HMI and PLC to Design a Universal Quality Inspection or Control Machine," *i-manager's Journal on Mechanical Engineering*, vol. 2, pp. 5-13, 2012, https://imanagerpublications.com/journalsfulldetails/10/JournalonMechanicalEngineering.

[35] M. D. Patil, "Robot Manipulator Control Using PLC with Position Based and Image Based Algorithm," *International Journal of Swarm Intelligence and Evolutionary Computation*, vol. 06, no. 1, pp. 1-8, 2017, https://www.walshmedicalmedia.com/open-access/robot-manipulator-control-using-plc-with-position-based-and-image-based-algorithm-2090-4908-1000154.pdf.

[36] C. Barz, T. Latinovic, Z. Erdei, G. Domide, and A. Balan, "Practical application with plc in manipulation of a robotic arm," *Carpathian Journal of Electrical Engineering*, pp. 78-86, 2014, https://doaj.org/article/d3911d2034e747b39b9fc8a339163a0d.

[37] A. Saeed, L. Wang, Y. Liu, M. Z. Shah, and Z. Y. Zuo, "Modeling and control of unmanned finless airship with robotic arms," *ISA Transactions*, vol. 103, pp. 103-111, 2020, https://doi.org/10.1016/j.isatra.2020.04.006.

[38] D. K. Thomsen, R. Søe-Knudsen, O. Balling, and X. Zhang, "Vibration control of industrial robot arms by multi-mode time-varying input shaping," *Mechanism and Machine Theory*, vol. 155, p. 104072, 2021, https://doi.org/10.1016/j.mechmachtheory.2020.104072.

[39] A. Hernandez-Sanchez, I. Chairez, I. Matehuala-Moran, M. Alfaro-Ponce, and A. Molina, "Trajectory tracking controller of a robotized arm with joint constraints, a direct adaptive gain with state limitations approach," *ISA Transactions*, vol. 141, pp. 276-287, 2023, https://doi.org/10.1016/j.isatra.2023.07.004.

[40] T. Gao, "Optimizing robotic arm control using deep Q-learning and artificial neural networks through demonstration-based methodologies: A case study of dynamic and static conditions," *Robotics and Autonomous Systems*, vol. 181, p. 104771, 2024, https://doi.org/10.1016/j.robot.2024.104771.

[41] S. Sha *et al*., "Research on force-position decoupling control technology of bonnet polishing of robotic arm," *Precision Engineering*, vol. 94, pp. 315-329, 2025, https://doi.org/10.1016/j.precisioneng.2025.03.012.

[42] J. Zhou, G. Zuo, S. Yu, S. Dong, and C. Liu, "Motion controller for multi-joint robotic arm with deep cascade gated Bayesian broad learning system," *Applied Mathematical Modelling*, vol. 138, p. 115792, 2025, https://doi.org/10.1016/j.apm.2024.115792.

[43] Y. Xiuxing and P. Li, "Enhancing trajectory tracking accuracy for industrial robot with robust adaptive control," *Robotics and Computer-Integrated Manufacturing*, vol. 51, pp. 97-102, 2018, https://doi.org/10.1016/j.rcim.2017.11.007.

[44] J. Hernandez *et al*., "Current Designs of Robotic Arm Grippers: A Comprehensive Systematic Review," *Robotics*, vol. 12, no. 1, p. 5, 2023, https://doi.org/10.3390/robotics12010005.

[45] L. Birglen and T. Schlicht, "A statistical review of industrial robotic grippers," *Robotics and Computer-Integrated Manufacturing*, vol. 49, pp. 88-97, 2018, https://doi.org/10.1016/j.rcim.2017.05.007.

[46] D. Yoon and Y. Choi, "Analysis of Fingertip Force Vector for Pinch-Lifting Gripper With Robust Adaptation to Environments," *IEEE Transactions on Robotics*, vol. 37, no. 4, pp. 1127-1143, 2021, https://doi.org/10.1109/TRO.2020.3045648.

[47] H. Liu, L. Zhao, B. Siciliano and F. Ficuciello, "Modeling, Optimization, and Experimentation of the ParaGripper for In-Hand Manipulation Without Parasitic Rotation," *IEEE Robotics and Automation Letters*, vol. 5, no. 2, pp. 3011-3018, 2020, https://doi.org/10.1109/LRA.2020.2974419.

[48] V. Babin and C. Gosselin, "Picking, grasping, or scooping small objects lying on flat surfaces: A design approach," *The International Journal of Robotics Research*, vol. 37, no. 12, pp. 1484-1499, 2018, https://doi.org/10.1177/0278364918802346.

[49] A. Ruo *et al*., "A low-cost 3D printed electromagnetic gripper for robotic arms," *Mechatronics*, vol. 110, p. 103374, 2025, https://doi.org/10.1016/j.mechatronics.2025.103374.

[50] V. S. Bathula, V. Mendi, S. Chinthamreddy, A. P. Kumar, and B. C. Bose, "Pick and place operation by collaborating electromagnetic and pneumatic gripper robots," *Materials Today: Proceedings*, 2023, https://doi.org/10.1016/j.matpr.2023.06.192.

[51] M. A. Rahman, A. Khan, T. Ahmed, and M. Sajjad, "Design, Analysis and Implementation of a Robotic Arm-The Animator," *International Journal of Engineering Research*, vol. 02, no. 10, pp. 298-307, 2013, https://www.ajer.org/papers/v2(10)/ZJ210298307.pdf.

[52] D. Rao, S. Vardhineni, N. Hemalatha, S. Mandava, and R. Kumar Mandava, "Design and development of robotic Manipulator's for medical surgeries," *Materials Today: Proceedings*, vol. 80, pp. 195-201, 2023, https://doi.org/10.1016/j.matpr.2022.11.242.

[53] F. J. Campa, M. Diez, J. Corral, E. Macho, S. Herrero, and C. Pinto, "Mechatronic design of a 3 degrees of freedom parallel kinematics manipulator with integrated force plate for human balance evaluation and rehabilitation☆," *Mechatronics*, vol. 105, p. 103278, 2025, https://doi.org/10.1016/j.mechatronics.2024.103278.

[54] C. Urrea, C. Domínguez, and J. Kern, "Modeling, design and control of a 4-arm delta parallel manipulator employing type-1 and interval type-2 fuzzy logic-based techniques for precision applications," *Robotics and Autonomous Systems*, vol. 175, p. 104661, 2024, https://doi.org/10.1016/j.robot.2024.104661.

[55] J. Denavit and R. S. Hartenberg, "A Kinematic Notation for Lower-Pair Mechanisms Based on Matrices," *Journal of Applied Mechanics*, vol. 22, no. 2, pp. 215-221, 2021, https://doi.org/10.1115/1.4011045.

[56] K. Dash, B. Choudhury, and S. Senapati, "Inverse Kinematics Solution of a 6-DOF Industrial Robot," *Soft Computing in Data Analytics*, pp. 183-192, 2019, https://doi.org/10.1007/978-981-13-0514-6_19.

[57] S. Aravinddhakshan, S. Apte, and S. Akash, "Neural Network Based Inverse Kinematic Solution of a 5 DOF Manipulator for Industrial Application," *Journal of Physics: Conference Series*, vol. 1969, p. pp 183-192, 2021, https://doi.org/10.1088/1742-6596/1969/1/012010.

[58] R. Köker, "A genetic algorithm approach to a neural-network-based inverse kinematics solution of robotic manipulators based on error minimization," *Information Sciences*, vol. 222, pp. 528-543, 2013, https://doi.org/10.1016/j.ins.2012.07.051.

[59] M. Anschober, R. Edlinger, R. Froschauer, and A. Nüchter, "Inverse Kinematics of an Anthropomorphic 6R Robot Manipulator Based on a Simple Geometric Approach for Embedded Systems," *Robotics*, vol. 12, no. 4, p. 101, 2023, https://doi.org/10.3390/robotics12040101.

[60] T. Ibarra-Pérez, J. M. Ortiz-Rodríguez, F. Olivera-Domingo, H. A. Guerrero-Osuna, H. Gamboa-Rosales, and M. D. Martínez-Blanco, "A Novel Inverse Kinematic Solution of a Six-DOF Robot Using Neural Networks Based on the Taguchi Optimization Technique," *Applied Sciences*, vol. 12, no. 19, p. 9512, 2022, https://doi.org/10.3390/app12199512.

[61] V. Kramar, O. Kramar, and A. Kabanov, "An Artificial Neural Network Approach for Solving Inverse Kinematics Problem for an Anthropomorphic Manipulator of Robot SAR-401," *Machines*, vol. 10, no. 4, p. 241, 2022, https://doi.org/10.3390/machines10040241.

[62] S. B. Šegota, N. Anđelić, V. Mrzljak, I. Lorencin, I. Kuric, and Z. Car, "Utilization of multilayer perceptron for determining the inverse kinematics of an industrial robotic manipulator," *International Journal of Advanced Robotic Systems*, vol. 18, no. 4, 2021, https://doi.org/10.1177/1729881420925283.

[63] F. Chen, H. Ju, and X. Liu, "Inverse kinematic formula for a new class of 6R robotic arms with simple constraints," *Mechanism and Machine Theory*, vol. 179, p. 105118, 2023, https://doi.org/10.1016/j.mechmachtheory.2022.105118.

[64] R. He, Y. Wang, and T. Li, "Design and control of the Six-DOF robotic manipulator," *Applied and Computational Engineering*, vol. 78, pp. 129-135, 2024, https://doi.org/10.54254/2755-2721/78/20240419.